

CAFE: Calar Alto Fiber-fed Echelle spectrograph

J. Aceituno¹, S.F Sánchez^{2,1}, F. Grupp³, J. Lillo⁴, M. Hernán-Obispo⁵, D. Benitez¹, L.M. Montoya¹, U. Thiele¹, S. Pedraz¹, D. Barrado^{1,4}, S. Dreizler⁶, and J. Bean⁶

¹ Centro Astronómico Hispano Alemán, Calar Alto, (CSIC-MPG), C/Jesús Durbán Remón 2-2, E-04004 Almería, Spain. e-mail: aceitun@caha.es.

² Instituto de Astrofísica de Andalucía (CSIC), Camino Bajo de Huétor s/n, Apto. 3004, E18080-Granada, Spain e-mail: sanchez@iaa.es.

³ Institut für Astronomie und Astrophysik der Universität München, Scheinerstr. 1, 81679 München, Germany.

⁴ Departamento Astrofísica, Centro de Astrobiología (INTA-CSIC), ESAC campus, P.O. Box 78, E-28691, Villanueva de la Cañada, Spain.

⁵ Universidad Complutense de Madrid, Av. Complutense s/n, 28040 Madrid, Spain.

⁶ University of Goettingen, Wilhelmsplatz 1 37073 Goettingen, Germany.

Received — ; accepted —

ABSTRACT

We present here CAFE, the Calar Alto Fiber-fed Echelle spectrograph, a new instrument built at the Centro Astronómico Hispano Alemán (CAHA). CAFE is a single fiber, high-resolution ($R \sim 70000$) spectrograph, covering the wavelength range between 3650-9800Å. It was built on the basis of the common design for Echelle spectrographs. Its main aim is to measure radial velocities of stellar objects up to $V \sim 13-14$ mag with a precision as good as a few tens of $m s^{-1}$. To achieve this goal the design was simplified at maximum, removing all possible movable components, the central wavelength is fixed, so the wavelength coverage; no filter wheel, one slit and so on, with a particular care taken in the thermal and mechanical stability. The instrument is fully operational and publicly accessible at the 2.2m telescope of the Calar Alto Observatory.

In this article we describe (i) the design, summarizing its manufacturing phase; (ii) characterize the main properties of the instrument; (iii) describe the reduction pipeline; and (iv) show the results from the first light and commissioning runs. The preliminary results indicate that the instrument fulfill the specifications and it can achieve the foreseen goals. In particular, they show that the instrument is more efficient than anticipated, reaching a $S/N \sim 20$ for a stellar object as faint as $V \sim 14.5$ mag in $\sim 2700s$ integration time. The instrument is a wonderful machine for exoplanetary research (by studying large samples of possible systems containing massive planets), galactic dynamics (high precise radial velocities in moving groups or stellar associations) or astrochemistry.

Key words. instrumentation: spectrographs, echelle | methods: observational | methods: data analysis | techniques: spectroscopic

1. Introduction

The Calar Alto Fiber-fed Echelle spectrograph (CAFE) is an instrument manufactured at the Centro Astronómico Hispano Alemán (CAHA) to replace FOCES (Pfeiffer 1992, Pfeiffer et al. 1998), the high-resolution echelle spectrograph at the 2.2m telescope of the observatory that was being operated during the period 1997-2010. CAFE was designed following the common concept of this kind of instrument e.g. Kaufer and Pasquini 1998, Stahl et al. 1999, Raskin et al. 2010, and therefore its design is very similar to that of FOCES e.g. Pfeiffer et al. 1992, Pfeiffer et al. 1994, Pfeiffer et al. 1998. The instrument was designed to achieve a spectral resolution of $R \sim 70000$, covering the wavelength range between 3850-9800Å. The main improvements of our design were focused on the increase of the stability and the sensitivity as much as possible. In particular, (i) we design a new camera, improving the one from FOCES; (ii) we use new branch, highly efficient and long-term stable fibers; (iii) the instrument has been located in an isolated room, thermalized and stabilized against vibrations (as we illustrate latter); (iv) most of the possible mobile parts in this kind of instruments have been substituted by fixed elements, to increase the stability of the system; and finally (v) a new more efficient CCD, with a smaller pixel has been acquired.

We expected that these improvements increase the efficiency and quality of the data with respect to its predecessor. The ultimate goal is that CAFE would achieve precisions of $\sim 10-20 m s^{-1}$ in the measurement of radial velocity of stellar objects down to $V \sim 14$ magnitudes. We are searching for the maximum radial velocity accuracy for a simple and unexpensive, fast track instrument. The goal was to produce a competitive instrument for several key areas such exoplanetary searches, including the Kepler candidates, and the exploitation of GAIA Perryman (2003). Thus, the $\sim 10-20 m s^{-1}$ is a compromise, and allows detailed studies of large samples of moderately faint stars. However, we would like to note that this instrument is built foreseen a single science case, but not to provide the community of users of the observatory with a facility to cover the same studied that were performed during the last 10 years using FOCES, improving the performance when feasible.

The instrument operates in a single mode, (as FEROS at ESO 1.52m Kaufer et al. (1997), HARPS at ESO 3.6m Pepe et al. (2000)) without any possible adjustment to increase either the resolution or the efficiency (to the contrary of other similar instruments with more movable elements, eg., FOCES, SOFIN at NOT 2.6m telescope Pronik (1995)).

The distribution of this article is the following one: In Section 2 we describe the main properties of the instrument. The details of the design and manufacturing are given in Section

3. The results from the tests performed during the First Light are shown in Section 4.1. Finally, the tests performed during the Commissioning and their results are shown in Section 4. A summary of the main characteristics of the instrument are included in Section 5.

2. Main properties of the instrument

CAFE is a stationary echelle spectrograph located at a remote laboratory in the dome building of the 2.2m telescope. This room is located below the main telescope structure, separated from the rest of the building, in order to reduce the effects of any mechanical vibration. The mechanical stability is increased by sophisticated pneumatic stabilization system installed in the optical bench manufactured by Newport Corporation (model I-2000-428). This guarantees a much better stability of the instrument, increasing its performance and accuracy for radial velocity measurements of fainter objects. The room has thick reinforced concrete walls, as been part of the main support of the telescope itself. This also provides a good thermal-isolation to the room. The instrument itself is separated ~18m from the Cassegrain focus of the telescope. The light is conducted by a single fiber and coupled to the focal plane with an improved version of the FOCES telescope module. It was manufactured by the company Ceramoptec and it has an stainless steel tube as outer protection and ETFE (Ethylene tetrafluoroethylene) with Kevlar for strain relief as inner protection tube.

The optical design of the instrument camera has been optimized, based on the knowledge acquired with FOCES. Based on modern optical software a better PSF could be achieved over the field of view. The system has been optimized for the size of the CCD in use. Finally, we equipped the instrument with a new CCD camera, an iKon-L of Andor Technologies company, with 2048x2048 pixels of 13.5 μm . This CCD has a better quantum efficiency, lower readout-noise and higher read-out speed than the currently used by FOCES. We expect to increase the efficiency by at least a ~10% using this detector.

As indicated before, the echelle image covers the visible spectral region from 3960 to 9500 nm, distributed in 84 orders. They are displayed in 84 spectral orders with full spectral coverage. Spectral orders are separated by 20 pixels in the blue and 10 pixels in the red. The maximum expected spectral resolution is $R = \lambda/\Delta\lambda = 67000$ with a 2 pixel resolution element. Table 1 summarizes the main properties of the instrument and Table 2 shows their references and manufacturers.

3. Detailed description of the instrument

3.1. Mechanical and thermal stability

As indicated before, the spectrograph is located inside a controlled thermal environment in order to minimize any possible thermal drifts during an observing night.

The upper part of the cabinet can be lifted up with a tackle anchored on the roof of the room, as shown in Fig.1, getting access to the optical bench. The enclosure is kept closed during the observations.

No electronic/mechanical control system is needed once the instrument is integrated, due to its design. The only active elements inside the cabinet are the focus stage of the camera and the shutter, which are kept disconnected during a normal operation. These issues add a better stability of the mechanical mounts installed on the optical bench.

Table 1. Basic features of CAFE.

Design	Echelle spectrograph
Telescope	Calar Alto 2.2m
Resolution	62000±5000 A
Wavelength	3960 - 9500 A
Sensitivity	SNR ~30 mag 14.5 and 2700sec
TELESCOPE MODULE	
Calibration lamps	Hal and ThAr
Entrance diaphragm	2.4 arcseconds (200 μm)
OPTICAL FIBER	
Type	Polymicro FBP100140170
Length	17.5m
Inner protection tube	ETFE with Kevlar for strain relief
Outer protection tube	stainless steel tube
Micro-lenses	N-F2, Both ends
SPECTROGRAPH	
Optical bench	2400 x 1200 x 203mm
Entrance slit width	100 μm
Grating	31.6 g/mm Blaze angle=63.9 degrees
Collimators	OAP1 $\lambda/20$ FL=60.0 D=10.0 OAD=7.0 OAP2 $\lambda/20$ FL=60.0 D=10.0 OAD=9.0
Prisms	LF5, Deviation angle 33 degrees
Camera	f/3
CCD back illuminated	2048x2048 pixels, 13.5 μm

(*): OAP: Off axis parabola, FL: focal length, OAD: off axis distance (respect to the center of the mirror. These magnitudes are in inches.

Table 2. Summary of the main elements of CAFE

Item	Manufacturer	Reference
CCD	Andor Technologies	iKON-L DZ936NBV
CCD cooling system	Solid State	XW-CHIL-150
Pneumatic isolators	NewPort Corp	I-2000-428
Collimators	NewPort Corp	OAP60-02-10Q OAP60-04-10SQ
Flat mirror	Bernhard Halle Nachff	–
Grating	NewPort Corp	53044ZD06-411E
Dispersion prisms	Prazisionsoptics Gera	10586.09.001
Custom mounts	Indicam technologies	–
Fiber optics	Ceramoptec	–
Camera optics	Prazisionsoptics Gera	–

Following the same philosophy, the entrance slit width of the spectrograph is fixed to 100 μm . The maximum expected spectrograph resolution for a 2.2m telescope is $R\phi = 60300$ with the slit width ϕ entered in arcseconds; at the 2.2 m telescope the standard slit width corresponds to 100 μm which subtends a 1.2 arcseconds angle on the sky. Thus a CCD chip with 2x2k pixels of 13.5 μm distance would yield a 2 pixel resolution of $R = 72000$ with increased spectral coverage. The selection of the slit's width matches with the average values of seeing at the Calar Alto observatory which corresponds to 0.89arcseconds Sánchez et al. (2007).



Fig. 1. The figure shows a view of an CAFE spectrograph with the cabinet opened. The internal optical elements are seen on the optical bench. The upper side is as straight as a die to avoid any small apertures that can break the thermal isolation. Due to that, the upper part has to be lifted up with the help of a tackle.

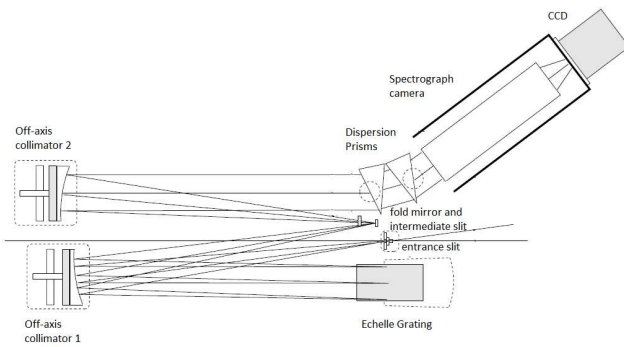


Fig. 2. Optical layout of the CAFE spectrograph with entrance slit, collimators, Echelle grating, folding mirror, prism/grism cross-disperser, and camera.

3.2. Optical design

The optical design of CAFE follows a white pupil concept, similar in many aspects to the one its precedent, FOCES (Baranne 1998). The optical layout is shown in Fig.2.

The light is collected by the telescope module (see Fig.3), which is attached to the Cassegrain focus of the telescope. It comprises a Halogen and Thorium-Argon lamps that are used as a continuum and wavelength calibration respectively, and an optical fiber that feeds the spectrograph. A motorized device allows to place any of the calibrations lamps in the optical path when they are needed. Their beams are designed to have roughly the same f -ratio ($f/8$) as the telescope beam to illuminate the entrance aperture with the same light cone. A 45° tilted mirror reflects the light into the fiber head and it might be rotated to accept light coming from any of the comparison lamps sources. Currently halogen and Thorium Argon lamps are available for flat field and wavelength calibration respectively.

Light entering into the fiber passes through a circular diaphragm which is located in a small tilted mirror just atop the fiber head. The diameter of such diaphragm is fixed to $200 \mu\text{m}$ that determines the angular field accepted by the fiber and corresponds to an sky area of 2.4arcseconds. This small tilted mirror

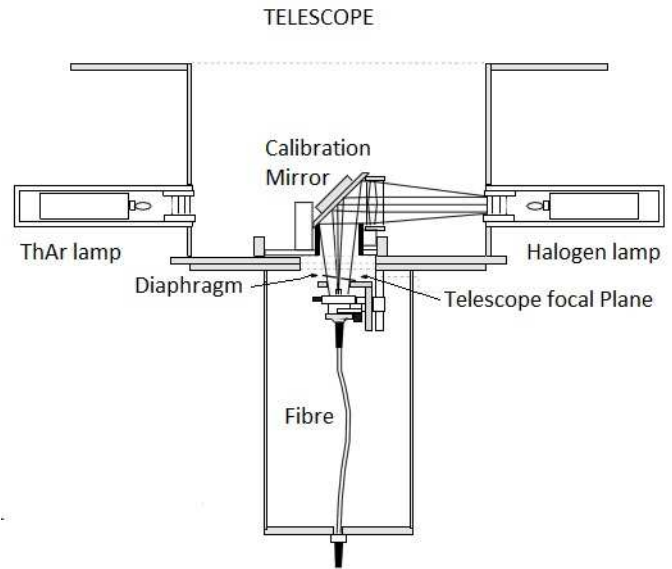


Fig. 3. The figure shows the telescope module. It is attached to the Cassegrain focus of the telescope and contains the calibration lamps, calibration mirror, a diaphragm and the fiber that brings the light to the spectrograph.

also allows guiding capabilities on the entrance aperture using the telescope guiding facilities.

Both ends of the fiber have a microlens glued to each surface and the corresponding principle is shown in Fig 4. As in the case of FOCES, a polymicro fiber was selected to be used with CAFE because it has been reported to have the least degradation among different available ones, e.g. Crause et al. (2008); Avila et al. (2006); Avila (1988).

A Fourier coupling is used. That means that the radial distribution of light in the telescope focal plane is transferred to an angular distribution on the fiber. As angular distribution of light couple to the fiber is preserved by the fiber (modulo FDR), the Fourier lens at the end recovers the radial information from the angular one.

The first element in the optical bench is the entrance slit used to recover the original resolution when the entrance diaphragm at the Cassegrain focus is widely open to let pass starlight in case of bad seeing. It is immediately aside of the folding mirror so the entrance slit and its spectral image are therefore very nearby as close as 0.9mm.

To follow a white pupil design, the spectrograph itself is collimated with two large off-axis parabolic mirrors. The 15 cm beam leaving the 31.6 lines/mm R2 echelle is refocused in the vicinity of a small folding mirror, used to reflect the converging beam in the intermediate slit image which passes a very efficient straylight baffle.

The cross-dispersion is achieved with two LF5 prisms installed on a symmetric tandem mounting which is under manual control. Instead of a low-order grating, a double prism for cross-dispersion is used, which accounts for a less strongly changing inter order distance, and it significantly reduces local straylight in the spectrum.

Finally, the beam is imaged with an $f3$ transmission camera onto a field centered on a back-illuminated CCD with $13.5 \mu\text{m}$ pixel size. The optical design of the instrument camera has been optimized, based on the knowledge acquired with FOCES. Based on modern optical software a better PSF could

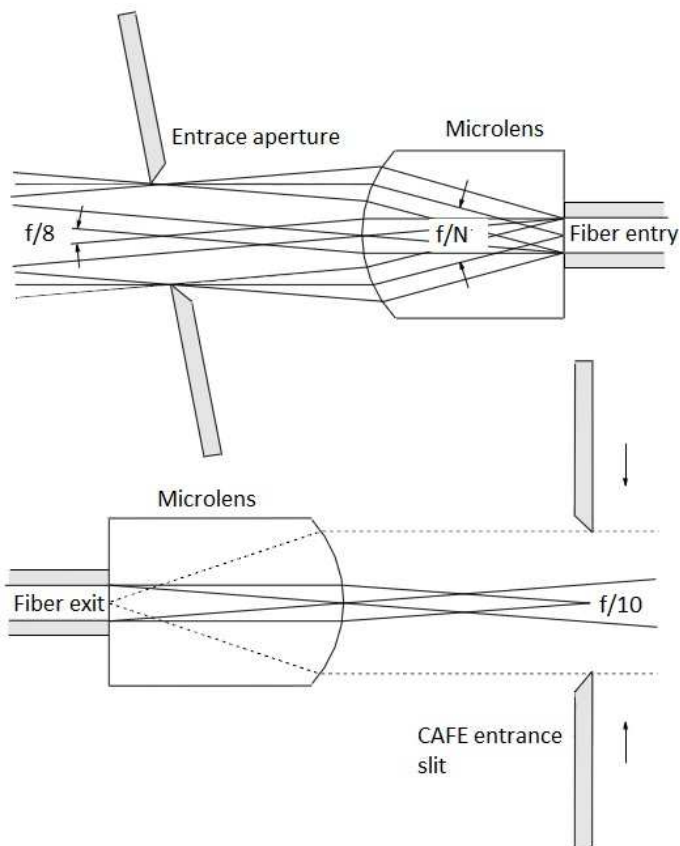


Fig. 4. Principle of working of the microlenses glued to the entrance and exit of the fiber. Upper panel: Fiber feed at the telescope module. Lower panel: Entrance at the spectrograph (Pfeiffer et al. (1998)).

be achieved over the field of view. The system has been optimized for the size of the CCD in use.

3.3. Pipeline

CAFE has been delivered with an automatic reduction pipeline. The main goal of this pipeline is to provide the user with a simple reduction of the data that can be used to test their quality during the observing run. Depending of the particularities of the science case, the data reduced using the pipeline could be used for science purpose or not, although this was not the main purpose of this package. The software is available for the community on request.

The reduction pipeline is based on R3D Sánchez (2006). Although the package was not originally designed to reduce Echelle data, these data share some of the basic properties of any fiber-fed spectrograph. The pipeline requires four basic entries to perform the reduction: (1) the science raw-frame, (2) a bias frame acquired during the night, (3) a continuum lamp frame, and (4) an arc-lamp frame (ThAr, in this case). The main reduction steps performed are the following: (i) the raw frames are corrected by the corresponding bias; (ii) the location of the orders across the cross-dispersion axis is determined based on the intensity peak of each order at the central pixel of the CCD. Then, each order is traced along the dispersion axis, using a similar algorithm; (iii) the science spectrum corresponding to each order is then extracted using a Gaussian extraction algorithm Sánchez (2006); Sánchez et al. (2012). A similar procedure is

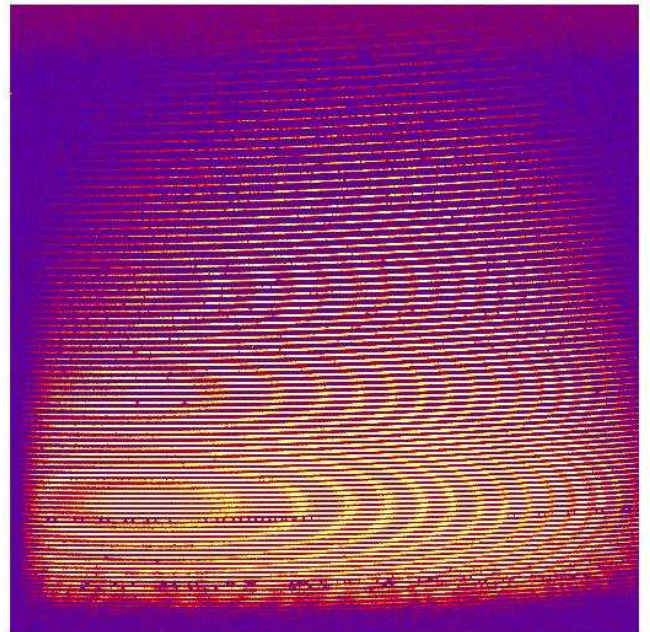


Fig. 5. Raw data of the first science frame taken with CAFE, on the star HR4728. The orders are displayed from red, at the bottom, to blue, at the top. For each order, the wavelength range runs from blue, at the left, to red, at the right.

used to extract the continuum and arc lamp spectra: (iv) The continuum extracted spectra are then used to create a master flat. For doing so, a low-order polynomial function is fitted to each continuum extracted spectrum, which is then divided by this smooth curve. The science frames are divided by this latter flat frame, correcting both the effects of the fringing and normalizing the transmission order-by-order. (v) Then, the wavelength calibration is derived for each order using the extract arc-lamp spectra. The identified emission lines are stored in an internal look-up-table (LUT)¹. It is used a five-order polynomial function to derive the wavelength calibration order-by-order. (vi) The wavelength calibration is applied to the science frames, normalizing the wavelength step to the nominal one order-by-order as shown in Table 3. (vii) Finally, a rough flux calibration is performed using a master-transmission curve derived during the commissioning runs.

4. Commissioning

4.1. First light

The first light of CAFE took place the night of the 24th of May 2011, when the instrument was for the first time installed in the telescope. The first observed science target was a bright ($V \sim 6$ mag) star, HR4728, selected by visibility and luminosity. The early tests performed along this night were focused on the identification of the orders and wavelength range covered by each one. The identification of the orders was a fundamental and not trivial task prior to the proper extraction and wavelength calibration of each frame.

First, the location of the projection of each order in the CCD, as seen in Fig.5 is determined using the corresponding tracing

¹ a summary of this LUT is shown in <http://www.caha.es/CAHA/Instruments/CAFE/cafe/orders2.pdf>

Table 3. CAFE: List of the clearly detected orders, including the order, the wavelength range and the spectral sampling (after re-sampling).

#	λ_{start} (Å)	λ_{end} (Å)	$\Delta\lambda/\text{pix}$ (Å/pix)	#	λ_{start} (Å)	λ_{end} (Å)	$\Delta\lambda/\text{pix}$ (Å/pix)	#	λ_{start} (Å)	λ_{end} (Å)	$\Delta\lambda/\text{pix}$ (Å/pix)
60	9432.964	9558.496	0.0645	88	6430.853	6516.885	0.0442	116	4877.880	4943.502	0.0337
61	9278.291	9401.792	0.0634	89	6358.568	6443.648	0.0437	117	4836.160	4901.236	0.0334
62	9128.607	9250.142	0.0624	90	6287.889	6372.039	0.0432	118	4795.146	4859.686	0.0331
63	8983.674	9103.305	0.0614	91	6218.764	6302.003	0.0427	119	4754.821	4818.833	0.0328
64	8843.271	8961.057	0.0605	92	6151.141	6233.490	0.0423	120	4715.168	4778.662	0.0326
65	8707.188	8823.185	0.0596	93	6084.972	6166.449	0.0418	121	4676.170	4739.154	0.0323
66	8575.229	8689.491	0.0587	94	6020.210	6100.835	0.0414	122	4637.811	4700.294	0.0321
67	8447.208	8559.787	0.0578	95	5956.812	6036.603	0.0410	123	4600.075	4662.066	0.0318
68	8322.953	8433.897	0.0570	96	5894.734	5973.708	0.0405	124	4562.947	4624.454	0.0316
69	8202.299	8311.657	0.0561	97	5833.936	5912.109	0.0401	125	4526.413	4587.443	0.0313
70	8085.092	8192.908	0.0554	98	5774.378	5851.768	0.0397	126	4490.459	4551.020	0.0311
71	7971.187	8077.504	0.0546	99	5716.023	5792.646	0.0393	127	4455.070	4515.170	0.0308
72	7860.446	7965.305	0.0538	100	5658.835	5734.706	0.0389	128	4420.234	4479.881	0.0306
73	7752.738	7856.180	0.0531	101	5602.779	5677.913	0.0386	129	4385.938	4445.138	0.0304
74	7647.942	7750.003	0.0524	102	5547.822	5622.233	0.0382	130	4352.168	4410.929	0.0301
75	7545.939	7646.658	0.0517	103	5493.932	5567.634	0.0378	131	4318.914	4377.243	0.0299
76	7446.621	7546.032	0.0510	104	5441.077	5514.086	0.0375	132	4286.164	4344.066	0.0297
77	7349.883	7448.020	0.0504	105	5389.229	5461.557	0.0371	133	4253.905	4311.388	0.0295
78	7255.624	7352.520	0.0497	106	5338.359	5410.019	0.0368	134	4222.128	4279.198	0.0293
79	7163.752	7259.438	0.0491	107	5288.440	5359.444	0.0364	135	4190.821	4247.485	0.0291
80	7074.176	7168.682	0.0485	108	5239.445	5309.805	0.0361	136	4159.974	4216.237	0.0289
81	6986.812	7080.168	0.0479	109	5191.348	5261.078	0.0358	137	4129.577	4185.446	0.0287
82	6901.579	6993.811	0.0473	110	5144.125	5213.236	0.0355	138	4099.620	4155.101	0.0285
83	6818.399	6909.536	0.0468	111	5097.753	5166.255	0.0352	139	4070.093	4125.192	0.0283
84	6737.199	6827.267	0.0462	112	5052.209	5120.114	0.0348	140	4040.988	4095.710	0.0281
85	6657.910	6746.933	0.0457	113	5007.470	5074.789	0.0345	141	4012.296	4066.645	0.0279
86	6580.464	6668.467	0.0452	114	4963.516	5030.259	0.0342	142	3984.007	4037.990	0.0277
87	6504.799	6591.805	0.0447	115	4920.326	4986.504	0.0340	143	3956.113	4009.736	0.0275

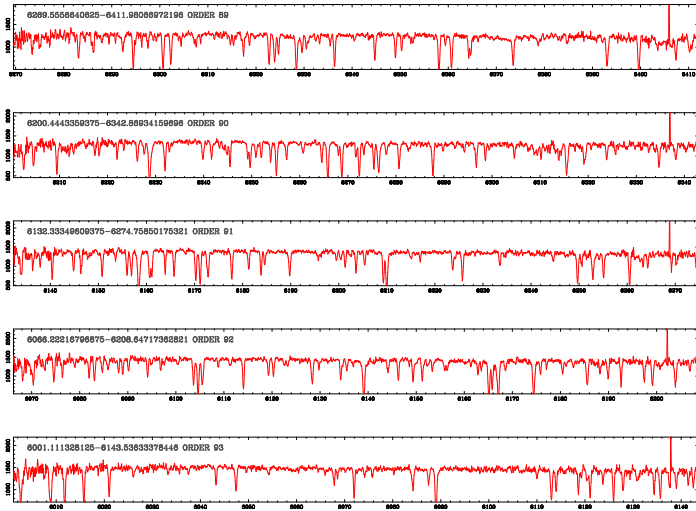


Fig. 6. Detail of a few orders of the extracted spectra of HR4728, reduced using the early version of the pipeline.

routines. Fig.7 shows a vertical cut of continuum lamp exposure used to trace these locations. The distribution of flux along the cross-dispersion axis corresponding to each of the orders is shown. For each one, the location of the peak intensity is indicated with a red (central pixel) and blue (hyperbolic centroid) cross.

The identification of the orders was done after tracing and extracting a ThAr frame (following the reduction steps explained in section 3.3).

Table 4 shows the 84 detected orders, including the Y-coordinate of the peak intensity of each order projected in the CCD at the central pixel in the X-axis, i.e., the pixel marked with a red cross in Fig.7. Table 3 shows, for each order, the wavelength range sampling, once normalized to a common spectral sampling per pixel.

4.2. Efficiency of the Instrument

The net efficiency of the instrument was derived by comparing the expected photons to obtain from a certain source with the real number of photons acquired by the instrument. For doing so, it was used the exposures on the calibration stars during the night of July 17th of 2011. We observed 5 different calibration stars along that night. The grammes were reduced using the pipeline (described latter), and finally it was extracted a (flux)-uncalibrated spectra for each of the orders, in counts. Then, counts were transformed into photoelectrons using the gain of the CCD for each wavelength ($n_{e,det}$).

To derive the number of expected photoelectrons it is required to use the known flux-calibrated spectra of the considered standard star. The observed spectrophotometric standard stars were all extracted from the Oke (1990) catalogue ², which flux density is provided in units of $10^{-16} \text{ Erg s}^{-1} \text{ \AA}^{-1} \text{ cm}^{-2}$. The amount of flux (F) at a certain wavelength λ , in a wavelength

² <http://www.caha.es/pedraz/SSS/Oke/oke.html>

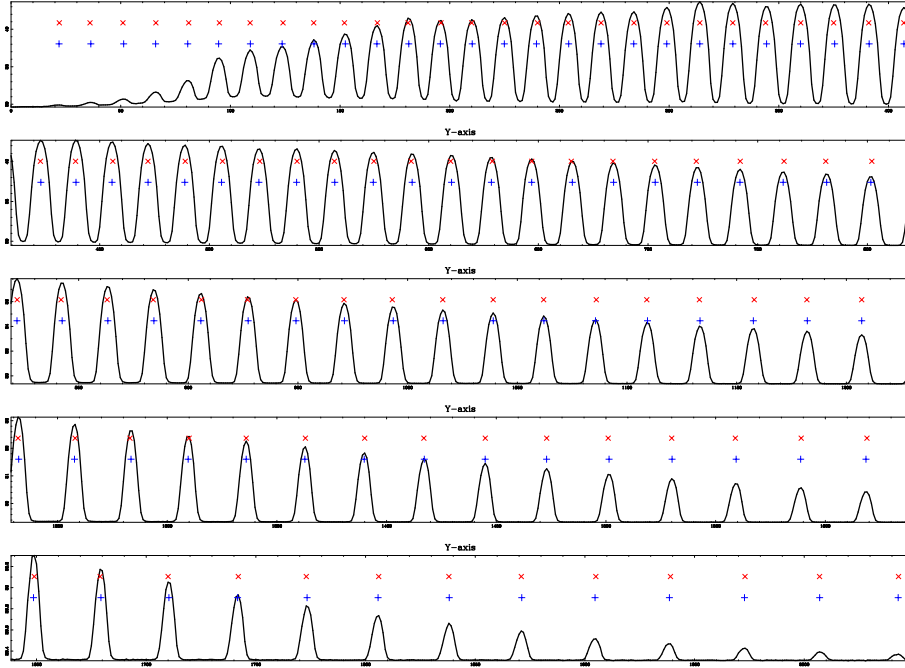


Fig. 7. Vertical section of a continuum exposure at the central X-axis pixel, showing the projection on the CCD of each order, from red wavelengths (top-left) to blue ones (bottom-right). The location of the peak intensity of each order is marked with a red cross (central pixel), and with a blue cross (centroid).

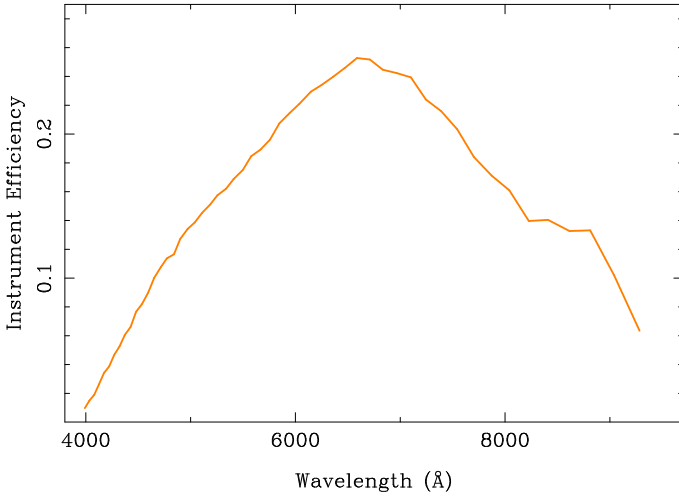


Fig. 8. Overall CAFE efficiency (including telescope) derived from the analysis of the calibration star taken during the commissioning run.

interval $\Delta\lambda$, of a star (or any other target), with flux density f_λ , collected by a telescope of collecting area (ΔS), in a time interval (Δt) is given by the formula:

$$F = f_\lambda \cdot \Delta S \cdot \Delta t \cdot \Delta\lambda$$

On the other hand, the energy of a single photon is:

$$f_{\text{photon}} = \frac{hc}{\lambda}$$

The ratio between both quantities, gives the number of *expected* photoelectrons ($n_{e,exp}$). This number can be compared di-

rectly with the number of *detected* photoelectrons, obtained from the reduced data as described before. Finally, the net efficiency of the instrument, as a function of the wavelength, is defined as:

$$efficiency = \frac{n_{e,det}}{n_{e,exp}}$$

Fig.8 shows the derived efficiency of the instrument (plus telescope and detector), as a function of the wavelength. CAFE is significantly more efficient than FOCES, at any wavelength range Pfeiffer et al. (1998). In comparison with other similar Echelle spectrographs, available at telescopes of a similar aperture, CAFE has a similar peak efficiency as FEROS (Guenther et al. (1999), Kaufer et al. (1999)), although this instrument is more efficient in the blue end. The main difference seems to be the efficiency of the CCD, which for FEROS has a coating whose efficiency changes from blue to red from one side to another across the CCD (ie., its coating is optimized for the wavelength range covered by each order). Therefore, a simple way to improve even more the efficiency of the instrument would be to acquire a similar CCD, although is not considered in the near future.

4.3. Instrumental Focus and Wavelength Resolution

One of the main goals in the design and manufacturing of CAFE was to achieve a better resolution than the one of its predecessor, with a better efficiency and stability. CAFE was designed to achieve a maximum resolution of $R \sim 70000$ (Sánchez et al. (2007)), in the optimal situation.

The resolution of the instrument is defined as the ratio between the wavelength λ and the minimum range of wavelengths that can be resolved $\Delta\lambda$. In practice, $\Delta\lambda$ is derived from the FWHM, in the spectral direction, of the emission lines of arc-lamps. Assuming that these lines are (in general), unresolved, the

Table 4. CAFE: List of detected orders.

#	Y pixel	#	Y pixel	#	Y pixel *
60	152	88	593	116	1182
61	167	89	611	117	1207
62	181	90	629	118	1232
63	196	91	647	119	1258
64	210	92	666	120	1283
65	225	93	685	121	1310
66	240	94	703	122	1336
67	254	95	723	123	1363
68	269	96	742	124	1390
69	284	97	762	125	1417
70	299	98	782	126	1445
71	314	99	802	127	1473
72	329	100	822	128	1501
73	345	101	843	129	1530
74	360	102	864	130	1559
75	376	103	884	131	1589
76	391	104	906	132	1618
77	407	105	927	133	1649
78	423	106	949	134	1679
79	439	107	971	135	1710
80	456	108	994	136	1741
81	472	109	1016	137	1773
82	489	110	1039	138	1805
83	506	111	1062	139	1837
84	523	112	1086	140	1870
85	540	113	1109	141	1905
86	557	114	1133	142	1938
87	575	115	1158	143	1972

(*) For each order we show the y-axis pixel at the x-axis center pixel in the CCD. The data showed here were obtained during the commissioning. An updated table can be found at <http://w3.caha.es/CAHA/Instruments/CAFE/index.html>

FWHM measures the instrumental resolution, i.e., the minimum wavelength elements to be resolved. Early measurements in the laboratory indicate that the FWHM of these emission lines were around ~ 2.2 pixels, which mostly corresponds to a resolution $R \sim 67000$ at the average wavelength sampled by the instrument ($\lambda 6500\text{\AA}$).

A detailed derivation of the spectral resolution can be done after a proper identification of the orders, the wavelength range covered by each of them, and the corresponding sampling ratio per pixel. Once reduced an arc-lamp exposure, using the pipeline described latter, each of the 336 identified arc emission lines are fitted with a one dimensional Gaussian function in both the dispersion and cross-dispersion directions, deriving the FWHM in both axis. The FWHM in the cross-dispersion axis illustrates how well each order is separated from the adjacent ones, and by which amount they are contaminated by cross-talk. Fig.9 shows the distribution of both FWHMs across the field-of-view of the CCD.

On the other hand, the FWHM in the dispersion axis is a direct measurement of the spectral resolution. Once it is derived the FWHM of each of the identified lines, a clipping algorithm rejects those values ($< 10\%$) that deviated more than 3σ of the mean one. The derived FWHM is multiplied by the step in wavelength per pixel and divided to the wavelength of the line, to derive the instrumental resolution (R).

Fig.10 shows the distribution of the spectral resolution along the wavelength derived from the first ThAr lamp observed the night of the 16th of June 2011. Similar distributions are found

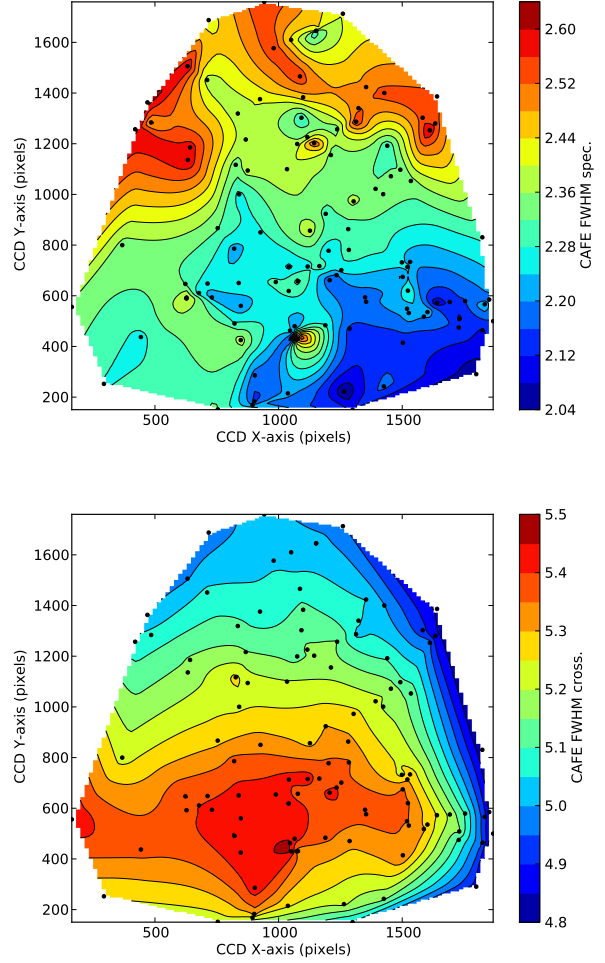


Fig. 9. CAFE: FWHM of the arc-lamp emission lines. Upper panel shows the distribution of the FWHM of the arc-lamp emission lines along the dispersion axis (X-axis), across the field-of-view of the CCD. Lower panel shows a similar distribution for the FWHM along the cross-dispersion axis.

for any of the arc calibration frames taken along the commissioning run. In average, the instrumental resolution estimated on real data corresponds to $\sim 63000 \pm 4000$. There is a clear trend in the resolution from the blue to the red range, with the resolution being ~ 60000 in the blue end ($\sim 4000\text{\AA}$), and about ~ 70000 in the red end ($\sim 9500\text{\AA}$). This median value is statistically dominated by the values at wavelengths bluer than $\sim 5500\text{\AA}$, where there are more identified arc lines. As anticipated, the resolution at the average wavelength of $\sim 6500\text{\AA}$ is ~ 65000 .

Following the specifications of the design, CAFE was built and calibrated to produce a similar accurate image quality at any position across the CCD. I.e., it was a goal of the design to have the same FWHM in the ThAr spots from blue to red arm at any order, at least in the spectral axis. A constant FWHM (in pixels) produces an unavoidable change in the resolution along the spectral range, as the one observed here.

This resolution is, in average, larger than the one that could be achieved by FOCES³. With that instrument, it was feasible to

³ http://www.caha.es/pedraz/Foces/spec_resol.html

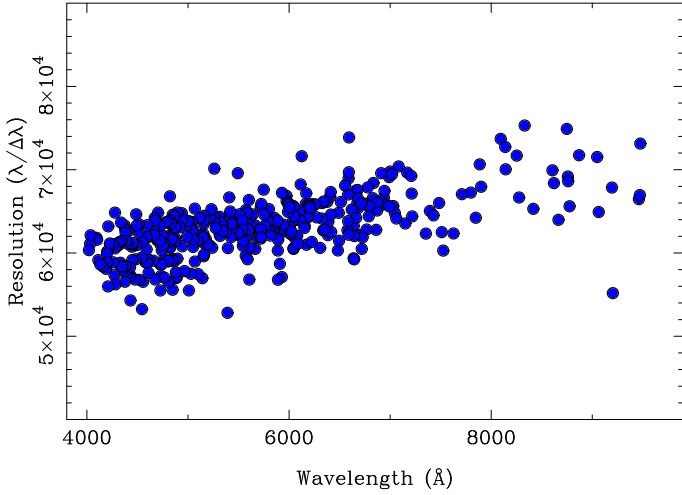


Fig. 10. CAFE: Wavelength resolution derived from the estimation of the FWHM of the identified ARC emission lines in the dispersion axis.

reach a resolution of about ~ 65000 only when observing with the narrowest slit width (with the consequent loss of signal-to-noise), and it was not feasible to achieve a better resolution above this value.

4.4. Stability of the Focus

CAFE was designed to stabilize the camera focus (and therefore the resolution) as much as possible. Due to that, compared with its predecessor, many moving elements have been replaced by fixed ones. To test if this goal has been achieved it is required to repeat the measurements described in Section 4.3 for different ARC-lamps exposures taken under different conditions.

So far, we got 34 ThAr ARC lamp frames along the commissioning run. We repeated the procedure described before for each of them, deriving the mean (and standard deviation) of the FWHMs values measured for each of them, and compacted one each other. Fig. 13 shows the distribution of these mean FWHMs along the time (upper panel) and along the internal temperature of the instrument (lower panel). It is important to note here that although the instrument is equipped with a thermal controlling system, this system was not operational during the Commissioning run. Therefore, any effect of the temperature on the focus (and the stability of the resolution) should be detected in this plot.

The average value of the FWHMs along the dispersion axis range yields between 2.3-2.35 pixels, without any significant variation either with the time and/or the temperature. The variation across the field is much larger (see Fig. 9) than any of possible detected variation along the time/temperature. In this regards, the goals of the design have been completely full-filled.

It is required to (1) do this analysis for any of the observed nights here after to feed the statistics with more data, and (2) repeat the analysis if the focus is redone.

Fig. 11 shows the high stability of CAFE along a 6 hours observing night on June 23rd, 2012. We used 43 spots in 14 ThAr arc images along the night to follow their centroid values (in the X and Y directions). The mean dispersion of the centroid position in the X-axis for the different images is 0.009 pixels while 0.010 pixels is found for the Y direction, resulting in a radial ve-

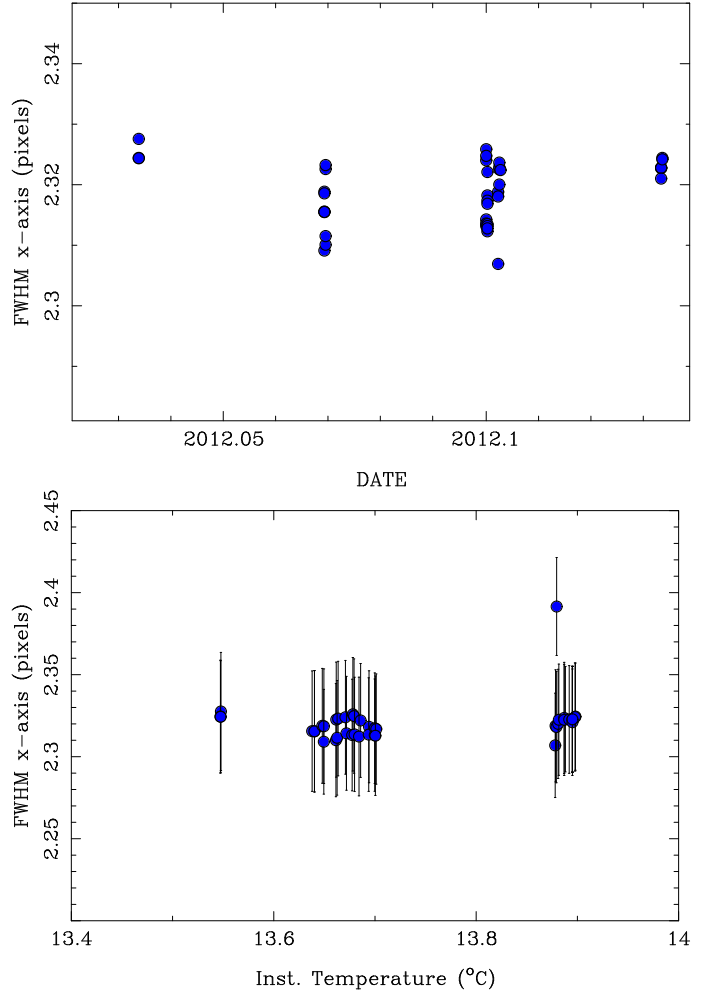


Fig. 13. CAFE: Stability of the spectral resolution. Upper panel shows the distribution of the average FWHM of the ARC emission lines along the dispersion axis (e.g., the one shown in Fig. 10), for the different ARC frames taken along the commissioning run. Lower panel shows a similar distribution along the internal temperature of the instrument, measured with the four sensors described in Section 3.1.

locity precision of around 18.5 m/s and 21.2 m/s, respectively. It is also important to note a slight dependence on the centroid position along the night. However, it can be easily corrected by using the closest ThAr arc to wavelength calibrate the science images and hence achieve the mentioned precisions. We detect different trends depending on each particular night so, if the scientific program requires high precision radial velocity measurements, we would strongly recommend to obtain arc calibrations prior and after each science image.

4.5. Signal-to-Noise

CAFE was designed to be more efficient than FOCES. For doing so new branch fibers, optics, higher-efficiency elements and less movable elements were included.

To determine if we have achieved this goal, we used the flux-calibrated spectra of the different objects observed during the commissioning run to derive the average S/N ratio (per spectral pixel). For doing so, an automatic procedure was included in

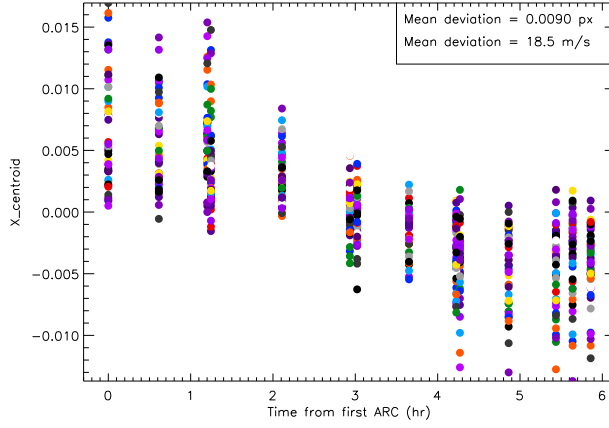


Fig. 11. Stability of CAFE along a 6 hours observing night on June 23rd, 2012. The mean dispersion of the centroid position in the X-axis for the different Th-Ar frames are shown. 43 spots, represented with different colors, have been used in 14 ThAr arc images to generate this figure.

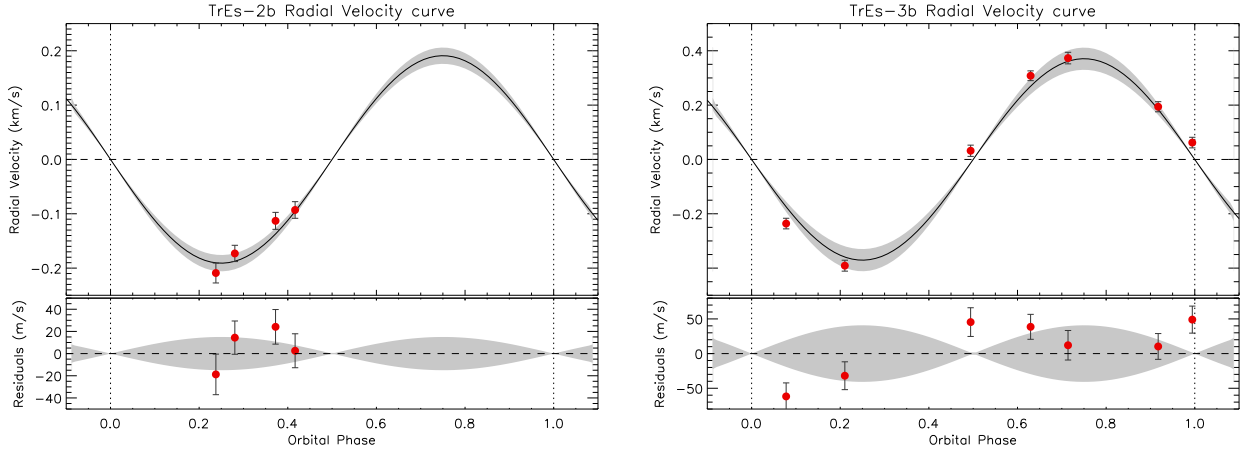


Fig. 12. Radial velocity curves for two well-known extra solar planets, TrEs-2b (*left-panel*), and TrEs-3b (*right-panel*), derived from the early measurements taken during the CAFE commissioning run. Red circles represent the derived values for the radial velocity. The black solid line represents the theoretical curve assuming the simple expression: $v_r = \frac{2\pi a}{P} \sin(i) \frac{M_p}{M_p + M_s} \sin(\phi)$ where a is the semi-major axis, P is the orbital period, i is the orbital inclination and ϕ is the orbital phase. The shaded region has been calculated by error propagation of the published values in the previous expression. The lower panel shows the residuals for the fit.

the CAFE pipeline, that compares the extracted signal, with the derived variance after propagating the different reduction steps.

Fig. 14 shows the theoretical curves derived from a exposure time calculator for CAFE. The achieved SNR as a function of time for a given magnitude has been included for the corresponding theoretical curve.

Table 5 shows the results of this S/N analysis, for all the targets observed along the commissioning run, including the date, the name of the target, the V-band magnitude and the S/N at the average wavelength of this band ($\sim 5500\text{\AA}$). However, a similar S/N, within a 20% is derived for the full wavelength range between 5000-6500 \AA , depending more on the shape of the continuum of the considered target (e.g stellar type) than in the properties of the instrument. These results can be directly compared with the ones derived for FOCES⁴. We highlight here the results derived for the G5 star with V-band magnitude of 6.9 mag, derived with FOCES, obtaining a S/N ~ 41 for a exposure time

of 60 sec. This can be compared with the result we obtain for HF151541, with CAFE, a $V \sim 7.1$ mag star, for which we obtain a S/N ~ 68 with a exposure time of 60 sec. The faintest object listed in the FOCES reference web-page, is a 0p star with a luminosity of $V \sim 10.5$ mag, for which it was obtained a spectra with a S/N ~ 25 with a exposure time of 600 seconds. A similar star, BD+25d4655, $V \sim 10.6$ mag, was observed with CAFE, for which we obtained a spectrum with a S/N ~ 45 , for with a similar exposure time ($t_{exp} \sim 600$ sec).

In average, the S/N derived by CAFE is twice larger than the one derived with FOCES for targets with similar luminosity and using similar exposure times.

Fig. 15 summarizes the results of this analysis, showing in two different representations the dependency of the S/N with the intrinsic brightness of the observed object and the adopted exposure time. Based on these results, the limiting magnitude of CAFE would be ~ 15 mag, for an exposure time of 1 hour, with

⁴ <http://www.caha.es/pedraz/Foces/signal.html>

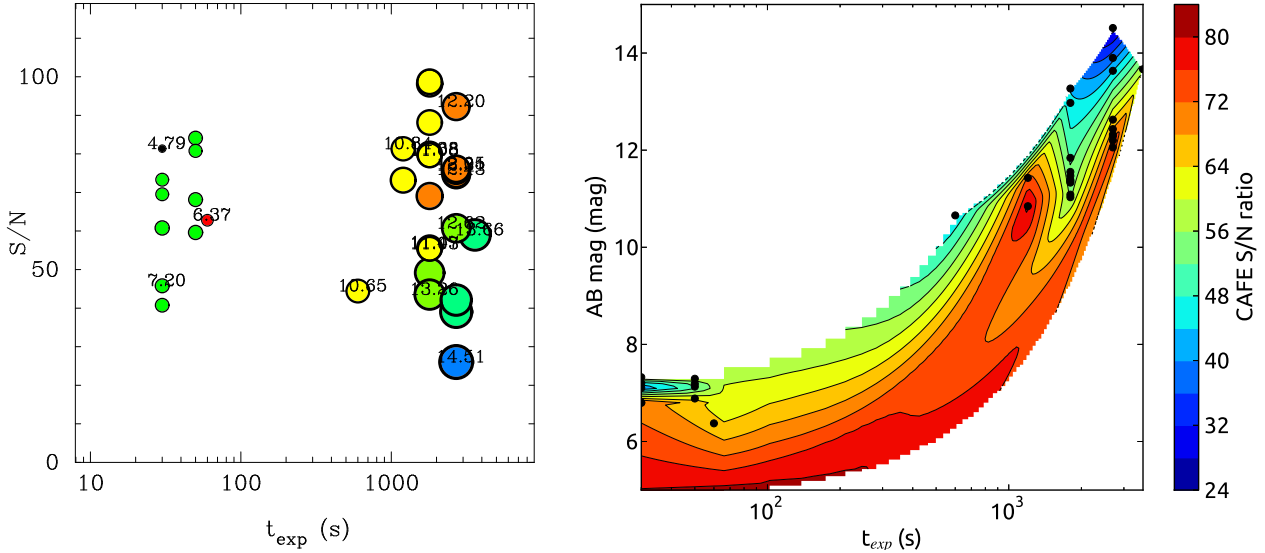


Fig. 15. CAFE: Results from the analysis of the S/N. Left panel shows the distribution of the S/N along the exposure time, for the different observed objects. Color/size of the plotted symbols indicate the brightness of the considered object. Right panel shows the S/N distribution as a function of the brightness and the exposure time.

Table 5. Summary of the Observed objects along the Commissioning nights

Date	Object Name	Exposure Time	AB (mag)	S/N
11-06-15 22:30:10	HAT-P-12b	2700	12.4	57.3
11-06-15 23:22:36	WASP-24b	1800	11.3	67.7
11-06-16 00:29:44	KOI-561B	3600	13.6	45.3
11-06-16 00:45:04	HD154345	30	6.8	56.3
11-06-16 00:49:41	HD154345	60	6.3	48.3
11-06-16 01:27:21	TrES-2b	1800	11.5	75.4
11-06-16 02:24:05	Tres-3b	2700	12.2	70.1
11-06-16 02:57:13	TrES-2b	1800	11.3	75.9
11-06-16 03:03:00	THD182572	30	4.7	62.5
11-06-17 21:13:45	HZ44	1800	11.8	53.0
11-06-17 21:46:51	Feige66	1200	10.8	62.5
11-06-17 22:14:10	BD+33d2642	1200	11.4	56.2
11-06-17 23:14:34	TrES-3b	2700	12.6	46.7
11-06-17 23:19:53	HD115404	30	6.7	53.4
11-06-17 23:35:51	HD139323	30	7.20	35.1
11-06-18 00:11:11	P330D	1800	12.9	37.7
11-06-18 00:52:22	TrES-2b	1800	11.4	42.7
11-06-18 01:04:29	HD151541	50	7.2	45.8
11-06-18 01:33:24	BD+25d4655	600	10.6	34.1
11-06-18 02:32:04	TrES-3b	2700	12.2	57.5
11-06-18 03:12:31	TrES-2b	1800	11.0	42.5
11-06-18 03:23:20	HD090404	50	7.1	64.6
11-06-18 20:58:34	P330D	1800	13.2	33.4
11-06-18 21:04:44	HD115404	30	7.1	31.3
11-06-18 22:03:56	TrES-3b	2700	12.3	58.2
11-06-18 23:00:47	Kepler-561	2700	13.8	30.0
11-06-18 23:35:28	TrES-2b	1800	11.3	61.4
11-06-18 23:44:03	HD139323	30	7.3	46.7
11-06-19 00:41:05	TrES-3b	2700	12.0	58.5
11-06-19 01:30:06	Kepler-561	2700	13.6	32.3
11-06-19 02:08:19	TrES-2b	1800	11.0	61.2
11-06-19 02:18:33	HD151541	50	7.1	52.3
11-06-19 03:12:25	Kepler-561	2700	14.5	20.0
11-06-19 03:25:07	HD190404	50	6.8	62.1

a S/N ratio of ~ 20 . We consider that the goal of providing an instrument more efficient than FOCES has been fulfilled.

These figures/tables should be fed with any additional information provided in any further observing run to derive much more accurate results/expectations.

4.6. Radial velocities measurements

Fig.11 shows the high stability of CAFE along a 6 hours observing night on June 23rd, 2012. We used 43 spots in 14 ThAr arc images along the night to follow their centroid values (in the X and Y directions). The mean dispersion of the centroid position in the X-axis for the different images is 0.009 pixels while 0.010 pixels is found for the Y direction, resulting in a radial velocity precision of around 18.5 m/s and 21.2 m/s, respectively. It is also important to note a slight dependence on the centroid position along the night. However, it can be easily corrected by using the closest ThAr arc to wavelength calibrate the science images and hence achieve the mentioned precisions. We detect different trends depending on each particular night so, if the scientific program requires high precision radial velocity measurements, we would strongly recommend to obtain arc calibrations prior and after each science image.

As it was said in previous sections, during the Commissioning run, we observed some already known planets in order to test the CAFE capabilities with real data. Spectra of parent stars TrEs-3 O'Donovan et al. (2007) and TrEs-2 O'Donovan et al. (2006) were acquired in different phases of their orbits.

The former system is composed by a $M_p \sin(i) = 1.91^{+0.06}_{-0.08} M_J$ planet orbiting a G-type star (TrES-3) of $M_s = 0.924^{+0.012}_{-0.04} M_\odot$. The physical and dynamical characteristics of this system causes a movement of the parent star around the center of masses with an amplitude of $K = 371 \pm 41$ m/s (error calculated during the orbit's quadrature). In Fig16, we show the observational points taken with CAFE after reducing the raw data with the pipeline explained in the previous section. Radial velocity for each spectra has been derived by cross-correlating the 50 orders with

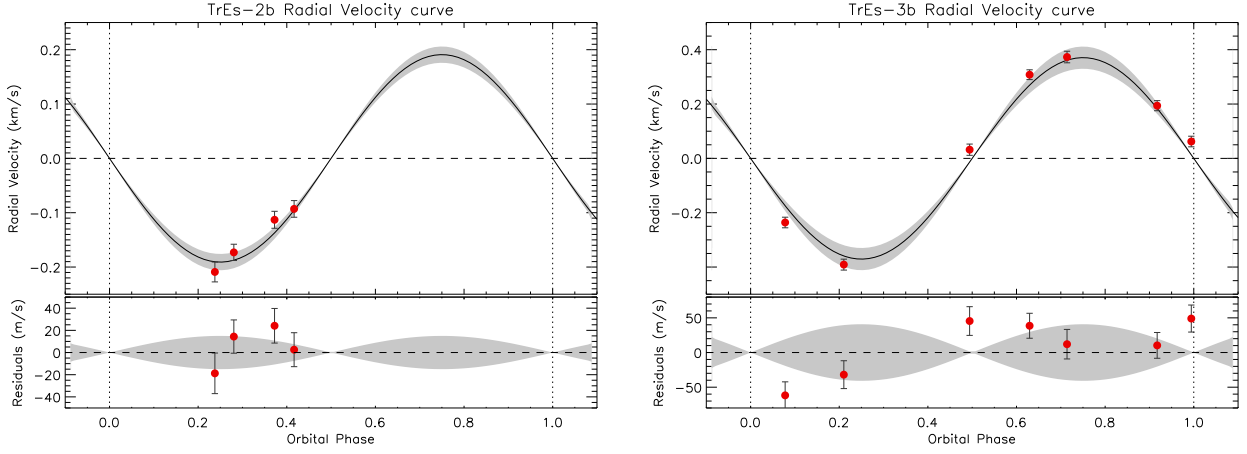


Fig. 16. Radial velocity curves for two well-known extra solar planets, TrEs-2b (*left-panel*), and TrEs-3b (*right-panel*), derived from the early measurements taken during the CAFE commissioning run. Red circles represent the derived values for the radial velocity. The black solid line represents the theoretical curve assuming the simple expression: $v_r = \frac{2\pi a}{P} \sin(i) \frac{M_p}{M_p + M_s} \sin(\phi)$ where a is the semi-major axis, P is the orbital period, i is the orbital inclination and ϕ is the orbital phase. The shaded region has been calculated by error propagation of the published values in the previous expression. The lower panel shows the residuals for the fit.

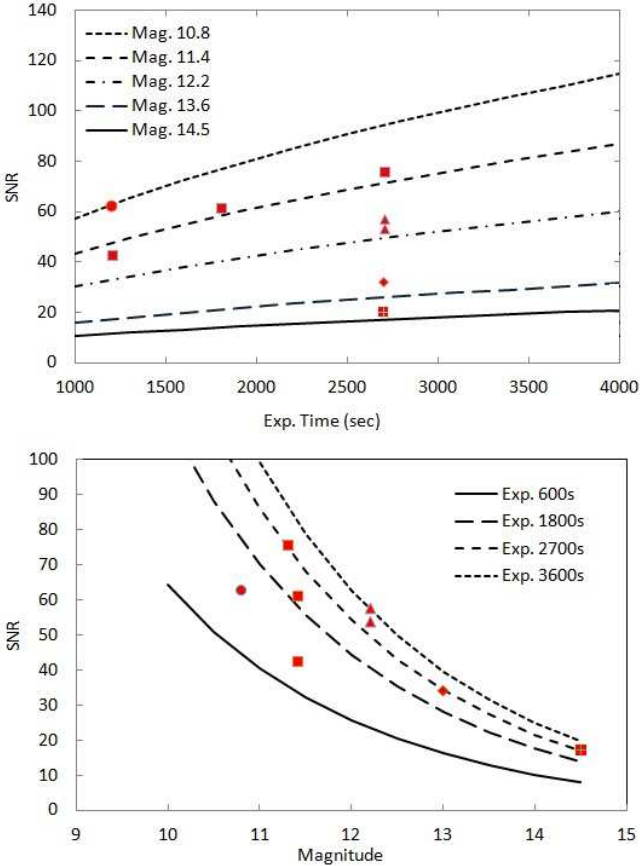


Fig. 14. Upper panel: The plot shows the SNR as a function of time for a given magnitude. Some experimental data for the corresponding magnitude have been overlapped to the theoretical curves for which magnitudes were derived. Lower panel: SNR is shown as a function of magnitude for different fixed exposure time. Same experimental data than in the upper case have been plotted to be consistent.

the highest signal to noise ratio with a solar spectrum⁵. When combining all the cross-correlation functions of the orders, we weightened them according to their FWHM. In the mentioned figure, we also plot the radial velocity curve according to the published parameters of the system⁶. A nice fit with the largest residuals being of the order of 50 m/s is obtained.

We proceed in the same manner for the second star, TrES-2, that hosted a planet lighter than TrES-3b. This planet is less massive than TrES-3b ($M_p \sin(i) = 1.253 \pm 0.052 M_J$) and orbits a heavier star of $M_s = 0.980 \pm 0.062 M_\odot$. Hence the amplitude of the radial velocity curve is significantly smaller, $K = 190 \pm 15$ m/s. Although, in this case, a slightly poor sampling of this curve was taken, we can see in Fig 11 that smaller residuals were obtained. Again, observed points with CAFE fit what is expected for this system, with residuals smaller than 20 m/s.

According to our observations of radial velocity standards, we find precisions of 22 m/s in the case of HD124292 if we remove the night-by-night trend (see Fig17). This trend could be cause by different effects such as stellar pulsation or night-by-night instrumental effects due to some small problems related to the arc lamp intensity stability. This is due basically to the optimal temperature required for the lamp to produce sharp emission lines, and not broader ones, which centroids are different. Only when the lamp is switched-on during the complete nights it is reached an optimal stability in the position of the arc-lamps. However, this is not feasible, due to the possible effects in stray-light.

Note that these radial velocity measurements have been determined by using high signal-to-noise spectra (greater than 80) of bright known standards and cross-correlating it with synthetic spectra of the same spectral type. The larger rms obtained in the case of TrEs-3b could be due among others to the fact that the Tres-3 spectra have lower signal-to-noise ratio (around 30).

⁵ www.bass2000.obspm.fr

⁶ Obtained from the www.exoplanet.eu website

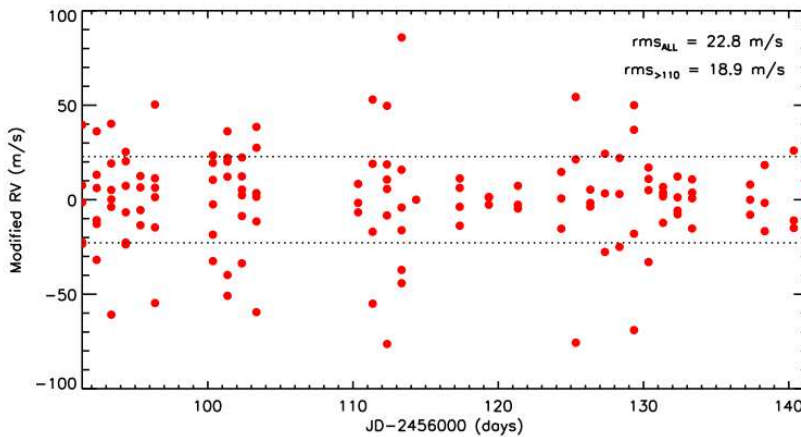


Fig. 17. RMS error of radial velocity measurements of the standard HD124292.

5. Summary and Conclusions

In this paper, we have presented the design, manufacturing and performance analysis of CAFE. We showed that the instrument was built according to the demanding requirements which resulted in an instrument of excellent stability and efficiency. First tests at the telescope were presented and lead to very encouraging results, which might be summarized as follows:

- The instrument is fully operational and publically accessible.
- The resolution estimated on real data corresponds to $62000 \pm 5000 \text{Å}$.
- Based on real observations, the limiting magnitude of CAFE would be ~ 15 mag, for an exposure time of 1 hour, with a S/N ratio of ~ 20 .
- Two known planets have been observed and their radial velocities measured to test the CAFE capabilities.
- The high stability of the instrument shows that a radial velocity precision about $\sim 20 \text{ m s}^{-1}$ might be achieved.

6. Acknowledgements

The authors thank the sub-programs of *Viabilidad, Diseño, Acceso y Mejora de ICTS*, ICTS-2008-24 and ICTS-2009-32, the PAI *Proyecto de Excelencia* P08-FWM-04319 and the funds of the PAI research group FQM360, and the MICINN program AYA2010-21161-C02-02, AYA2010-22111-C03-03, CDS2006-00070 and PRICIT-S2009/ESP-1496. We are grateful to all the Calar Alto staff and in particular to E. de Guindos, E. de Juan for the computer support, to S. Reinhart, M. Pineda, A. Garcia and J. Garcia who worked out during the mechanical assembling; to N. Vico, L. Hernandez, J. F. Lopez and J. Marin for their contributions to the new electronic controller and V. Gomez, M. Aguila, R. Lopez who their contributions to the preparation of the room that holds the instrument. We also want to thanks to the referee, which comments have improved this manuscript.

References

- Avila, G. 1988, in *Astronomical Society of the Pacific Conference Series*, Vol. 3, *Fiber Optics in Astronomy*, ed. S. C. Barden, 63–73
- Avila, G., Singh, P., & Albertsen, M. 2006, in *Society of Photo-Optical Instrumentation Engineers (SPIE) Conference Series*, Vol. 6269, *Society of Photo-Optical Instrumentation Engineers (SPIE) Conference Series*

- Crause, L., Bershady, M., & Buckley, D. 2008, in *Society of Photo-Optical Instrumentation Engineers (SPIE) Conference Series*, Vol. 7014, *Society of Photo-Optical Instrumentation Engineers (SPIE) Conference Series*
- Guenther, E., Stecklum, B., & Klose, S., eds. 1999, *Astronomical Society of the Pacific Conference Series*, Vol. 188, *Optical and Infrared Spectroscopy of Circumstellar Matter*
- Kaufer, A., Stahl, O., Tubbesing, S., et al. 1999, *The Messenger*, 95, 8
- Kaufer, A., Wolf, B., Andersen, J., & Pasquini, L. 1997, *The Messenger*, 89, 1
- O’Donovan, F. T., Charbonneau, D., Bakos, G. Á., et al. 2007, *ApJ*, 663, L37
- O’Donovan, F. T., Charbonneau, D., Mandushev, G., et al. 2006, *ApJ*, 651, L61
- Pepe, F., Mayor, M., Delabre, B., et al. 2000, in *Society of Photo-Optical Instrumentation Engineers (SPIE) Conference Series*, Vol. 4008, *Society of Photo-Optical Instrumentation Engineers (SPIE) Conference Series*, ed. M. Iye & A. F. Moorwood, 582–592
- Perryman, M. 2003, in *Astronomical Society of the Pacific Conference Series*, Vol. 298, *GQAIA Spectroscopy: Science and Technology*, ed. U. Munari, 3
- Pfeiffer, M. J., Frank, C., Baumüller, D., Fuhrmann, K., & Gehren, T. 1998, *A&AS*, 130, 381
- Pronik, V. I. 1995, *Izvestiya Ordena Trudovogo Krasnogo Znameni Krymskoj Astrofizicheskoy Observatorii*, 89, 111
- Sánchez, S. F. 2006, *Astronomische Nachrichten*, 327, 850
- Sánchez, S. F., Aceituno, J., Thiele, U., Pérez-Ramírez, D., & Alves, J. 2007, *PASP*, 119, 1186
- Sánchez, S. F., Kenicutt, R. C., Gil de Paz, A., et al. 2012, *A&A*, 538, A8

